Journal of the Korea Concrete Institute
Vol.15 No.5, pp.747-758, October, 2003

Effect of Confined High-Strength Concrete Columns

Kyung-Oh Van[1], Hyun-Do Yun[1]*, and Sun-Kyoung Hwang[2]

[1] Dept. of Architectural Engineering, Chungnam National University, Daejeon, 305-764, Korea
[2] Dept. of Architecture, Woosong University, Daejeon, 300-718, Korea

(Received May 16, 2003; Accepted September 23, 2003)

Abstract

The moment-curvature envelope describes the changes in the flexural capacity with deformation during a nonlinear analysis. Therefore, the moment-curvature analysis for reinforced concrete columns, indicating the available flexural strength and ductility, can be conducted providing the stress-strain relation for the concrete and steel are known. The moments and curvatures associated with increasing flexural deformations of the column may be computed for various column axial loads by incrementing the curvature and satisfying the requirements of strain compatibility and equilibrium of forces. Clearly it is important to have accurate information concerning the complete stress-strain curve of confined high-strength concrete in order to conduct reliable moment-curvature analysis that assesses the ductility available from high-strength concrete columns. However, it is not easy to explicitly characterize the mechanical behavior of confined high-strength concrete because of various parameter values, such as the confinement type of rectilinear ties, the compressive strength of concrete, the volumetric ratic and strength of rectangular ties. So a stress-strain model is developed which can simulate complete inelastic moment-curvature relations of high-strength concrete columns.

Keywords* : *moment-curvature, confined concrete, stress-strain model, high-strength concrete

1. Introduction

High-strength concrete (HSC) is now readily available for various practical applications such as bridges, offshore platforms, and buildings, as a result of ongoing progress in concrete technology. HSC offers many advantages, including excellent mechanical performance and ductility, which could result in initial and long-term cost reduction. HSC, however, is more brittle than conventional normal strength concrete (NSC).

Nonetheless, it has been shown that HSC columns can be having in a ductile manner under certain conditions. Hence, ACI-ASCE Committee 441[1] pointed out that columns subjected to axial-load less than 20% of column axial load capacity exhibited a good level of ductility when confined according to current ACI confinement requirements. The scientific community has not yet reached a consensus on required confinement reinforcement for ductile HSC columns. This can be limited number of tests on column under cyclic flexure and significant axial compression, specifically with axial-load in the range of 20 to 50 % of column axial-load capacity. It has also been shown that the confinement mechanism was not described properly by exiting models. Therefore, in seismically active regions, structural engineers tend to avoid using HSC.

In the first part of this research, a stress-strain confinement model is developed which can simulate complete inelastic moment-curvature relations of high-strength reinforced concrete columns. By analyzing the experimental data by multi-linear regression methods using SPSS program,[2] this study proposes regression equations to determine the peak stress and its corresponding strain of confined concrete expressed by tie stress, confinement effectiveness coefficient, the strength of concrete, the configuration of ties, and the rest variables. The second part of this research is to present modeling and parametric studies on moment-curvature relation of HSC columns subject to axial and horizontal load. Parametric studies are performed examine the effects of constituent material properties as well as topological arrangement of arrangement of reinforcements on moment- curvature relations HSC columns.

* *Corresponding author*
Tel.: +82-42-821-5622; Fax.: +82-42-823-9467
E-mail address:wiseroad@cnu.ac.kr

2. Constitutive model for confined HSC

2.1 Effective confinement pressure

The determination of the strength and ductility of confined concrete is based on the computation of effective confinement pressure, which depends on the stress in the transverse reinforcement at maximum strength of confined concrete, and on the effectively confined concrete area.

Where, it is difficult to exactly determine the tie stress. However the tie stress is related to the volumetric ratio of lateral ties, the confinement effectiveness coefficient, and other variables. In this paper, the tie stress is related to the volumetric ratio of lateral ties, the confinement effectiveness coefficient, and other variables. By applying the multi-linear regression method with the experimental results, shown in Table 1, it is computed the stress in the transverse reinforcement at maximum strength of confined HSC;

$$f_{hcc}=3.335\left(\frac{f_{yh}}{0.85f_{ck}}\right)-21.74\left(\frac{100}{s'}\right)-189.952\rho_{sl(\%)}-43.565\rho_{s(\%)} \\ +763.379K_e+37.332\rho_s f_{yh}-10.079K_e\rho_s f_{yh}-229.313 \quad (1)$$

2.2 Strength enhancement factor

The magnitude of the strength enhancement is a function of the volumetric ratio of lateral ties, the confinement effectiveness coefficient, and the stress in ties at maximum strength of confined concrete as important parameters to calculate the strength enhancement factor. By applying the multi-linear regression method with the experimental results, shown in Table 2, the strength enhancement is expressed by;

$$K_s=7.129\times10^{-6}(K_e\rho_{s(\%)}f_{hcc}) \\ +0.01386\left(K_e\rho_{s(\%)}\left(\frac{f_{hcc}}{f_{co}}\right)\right)+1.106 \quad (2)$$

2.3 Ductility for confined HSC

A regression analysis was performed on the test results of Chung (1997, 1998)[3,4], Shin (2002)[5,6], Lee (1990),[7] Sheikh (1980)[8] and Lim (1992)[9] to find the peak strain of confined concrete, and strain corresponding to 85% of peak stress of confined concrete on descending branch.

Table 1 Comparison of experimental and analytical f_{hcc} values

Specimens	f_{cu} MPa	f_{yh} MPa	$(f_{hcc})_{Exp}$ MPa	$(f_{hcc})_{Exp}/(f_{hcc})$①	$(f_{hcc})_{Exp}/(f_{hcc})$②	$(f_{hcc})_{Exp}/(f_{hcc})$③	Specimens	f_{cu} MPa	f_{yh} MPa	$(f_{hcc})_{Exp}$ MPa	$(f_{hcc})_{Exp}/(f_{hcc})$①	$(f_{hcc})_{Exp}/(f_{hcc})$②	$(f_{hcc})_{Exp}/(f_{hcc})$③
ㄱ-L6-100	14.7	545.2	281.4	0.94	0.73	0.52	ㄱ-2A1-1	37.5	481.5	358.5	0.91	1.03	0.74
ㄱ-L6-55	14.7	545.2	368.7	0.85	0.68	0.68	ㄱ-2A1H-2	37.0	268.1	255.1	0.79	0.95	0.95
ㄱ-L6-30	14.7	545.2	527.6	1.06	0.97	0.97	ㄱ-4CI-3	36.4	552.7	399.9	0.86	1.17	0.72
ㄱ-L8-100	14.7	535.4	313.8	0.98	0.59	0.59	ㄱ-4CIH-4	36.7	287.3	282.7	0.74	1.06	0.98
ㄱ-L8-30	14.7	535.4	442.3	0.76	0.83	0.83	ㄱ-4C6-5	35.0	481.5	499.9	1.04	1.04	1.04
ㄱ-M6-100	38.2	545.2	299.1	1.42	1.07	0.55	ㄱ-4C6H-6	34.3	268.1	262.0	0.81	0.98	0.98
ㄱ-M6-55	38.2	545.2	210.8	0.61	0.46	0.39	ㄱ-4A3-7	40.9	503.4	455.1	1.16	0.90	0.90
ㄱ-M8-100	38.2	535.4	198.1	0.86	0.56	0.37	ㄱ-4A4-8	40.8	528.0	420.6	0.93	0.80	0.80
ㄱ-M8-55	38.2	535.4	198.1	0.53	0.37	0.37	ㄱ-4A5-9	40.5	361.2	344.7	1.19	0.95	0.95
ㄱ-M6-30	38.2	535.4	325.6	0.73	0.61	0.61	ㄱ-4A6-10	40.7	459.6	455.1	1.10	0.99	0.99
ㄱ-H6-100	40.6	545.2	263.8	1.27	0.93	0.48	ㄱ-4C3-11	40.7	459.6	358.5	0.98	0.86	0.78
ㄱ-H6-55	40.6	545.2	273.6	0.80	0.62	0.50	ㄱ-4C3-12	40.8	719.6	458.8	0.80	0.65	0.65
ㄱ-H6-30	40.6	545.2	344.2	0.85	0.63	0.63	ㄱ-4A1-13	31.3	528.0	475.7	1.09	1.21	0.90
ㄱ-H8-100	40.6	535.4	232.4	1.02	0.66	0.43	ㄱ-2A5-14	31.5	448.7	427.5	1.19	0.95	0.95
ㄱ-H8-55	40.6	535.4	220.6	0.59	0.41	0.41	ㄱ-2A6-15	31.7	481.5	379.2	0.89	0.79	0.79
ㄱ-H8-30	40.6	535.4	440.3	0.99	0.82	0.82	ㄱ-2C1-16	32.5	667.6	589.5	1.18	1.51	0.88
ㄱ-L8D-30	18.1	505.0	534.5	1.14	1.06	1.06	ㄱ-2C5-17	32.9	459.6	348.2	0.94	0.76	0.76
ㄱ-L8C-30	18.1	565.8	565.8	1.11	1.00	1.00	ㄱ-2C6-18	33.1	528.0	551.6	1.08	1.04	1.04
ㄱ-L8D-50	18.1	558.0	558.0	1.15	1.00	1.00	ㄱ-4B3-19	33.4	459.6	399.9	1.08	0.87	0.87
ㄱ-L12R-70	18.1	580.6	580.6	0.99	1.00	1.00	ㄱ-4B4-20	34.7	517.1	544.7	1.10	1.05	1.05
ㄱ-M8D-30	29.7	505.0	531.5	1.23	1.05	1.05	ㄱ-4B6-21	35.5	481.5	489.5	1.03	1.02	1.02
ㄱ-M8D-50	29.7	558.0	558.0	1.31	1.00	1.00	ㄱ-4D3-22	35.5	459.6	386.1	1.02	0.84	0.84
ㄱ-H8D-30	47.9	505.0	565.8	1.39	1.12	1.12	ㄱ-4D4-23	35.9	517.1	530.9	1.12	1.03	1.03
ㄱ-H8D-50	47.9	558.0	518.8	1.30	0.93	0.93	ㄱ-4D6-24	35.9	481.5	475.7	1.03	0.99	0.99
ㄱ-H12R-70	47.9	580.6	568.8	1.11	0.98	0.98	Average				1.00	0.89	0.81
ㄱ Chung (1997, 1998) ㄱ Sheikh (1980)							Standard deviation				0.198	0.214	0.214

① Van and Yun (2003) ㄱ Cusson and Paultre (1995) ㄱ Saatcioglu and Razvi (1999)

It is suggested in Ref. [10] that all the remaining characteristic points on stress-strain curve can be reasonably approximated as a function of K_s. The following expressions are used for these characteristic points. The following peak strain ratio is calculated from Eq. (3).

$$\varepsilon_{cc}/\varepsilon_{co} = 21.5(K_s - 1)\left(\frac{K_e \rho_s f_{hcc}}{0.85 f_{ck}}\right) + 0.09912(K_s - 1)\left(\frac{f_{hcc}}{0.85 f_{ck}}\right) - 0.0428(K_e \rho_s f_{hcc}) + 0.949 \quad (3)$$

The following 85% of peak strain ratio is calculated from Eq. (4).

$$\varepsilon_{c85c}/\varepsilon_{co} = 136.893\left(0.15 K_s\left(K_e \rho_s \frac{f_{hcc}}{0.85 f_{ck}}\right)\right) + 0.187\left(0.15 K_s\left(\frac{f_{hcc}}{0.85 f_{ck}}\right)\right) - 0.15(K_e \rho_s f_{hcc}) + 0.826 \quad (4)$$

Where, ε_{co} is a function of concrete strength, this expression for ε_{co} was suggested by Setunge (1993),[11] by measuring the strain at maximum stress of concrete cylinders, with and without active confinement. The value of E_c is the Young's Modulus of concrete which can be taken as $9500(f_{ck})^{0.3}$ (MPa) in accordance with the recommendation by Setunge (1993).[11]

$$\varepsilon_{co} = \frac{4.26}{\sqrt[4]{f_{ck}}}\frac{f_{ck}}{E_c} \quad (5)$$

The strain corresponding to 50% of peak stress of confined concrete on descending branch is defined as the useful compressive strain limit for confined concrete. The limiting strain was observed to be close to the concrete axial strain corresponding to the first hoop fracture. Besides the ratio, $\varepsilon_{c50c}/\varepsilon_{co}$, is another indication of ductility index of confined concrete.

Table 2 Properties and results of specimens

Specimen	f_{cu} Mpa	f_{yh} Mpa	ρ_s %	K_s	ε_{cc}	ε_{c85c}	Specimen	f_{cu} Mpa	f_{yh} Mpa	ρ_s %	K_s	ε_{cc}	ε_{c85c}
¨-M6-100	38.1	545.2	0.70	1.10	0.0028	0.0038	¯-USC-F-12	86.7	440.0	5.01	1.31	0.0079	0.0160
-M6-55	38.1	545.2	1.20	1.30	0.0030	0.0057	¯-HCB1-3-4	38.1	472.7	2.73	1.43	0.0102	0.0176
-M6-30	38.1	545.2	2.20	1.46	0.0088	0.0134	¯-HCB2-3-4	38.1	472.7	1.36	1.13	0.0068	0.0142
¨-M8-100	38.1	535.4	1.20	1.11	0.0029	0.0034	¯-HCC1-4-4	38.1	472.7	2.73	1.50	0.0125	0.0194
¨-M8-55	38.1	535.4	2.20	1.35	0.0037	0.0069	¯-HCC2-4-4	38.1	472.7	1.36	1.16	0.0085	0.0208
¯-M8-30	38.1	535.4	4.10	1.65	0.0057	0.0120	¯-HCD1-3-4	38.1	472.7	2.73	1.56	0.0138	0.0199
¨-H6-100	50.7	545.2	0.70	0.97	0.0020	0.0065	¯-HCD2-3-4	38.1	472.7	1.36	1.34	0.0078	0.0134
¨-H6-55	50.7	545.2	1.20	1.10	0.0028	0.0054	¯-HCE-4-4	38.1	472.7	2.73	1.28	0.0121	0.0215
¨-H6-30	50.7	545.2	2.20	1.29	0.0034	0.0065	¯-HCF1-3-4	38.1	472.7	2.73	1.29	0.0120	0.0182
¯-H8-55	50.7	535.4	2.20	1.19	0.0037	0.0074	¯-HCF2-3-4	39.3	472.7	1.36	1.14	0.0089	0.0160
¨-H8D-30	56.4	505.0	2.30	1.55	0.0032	0.0110	¯-2A1-1	37.5	481.5	0.80	1.18	0.0036	0.0060
¨-H8C-30	56.4	565.8	2.30	1.46	0.0049	0.0090	¯-2A1H-2	37.0	268.1	0.80	1.26	0.0048	0.0098
¨-H8D-50	56.4	558.0	2.30	1.57	0.0057	0.0080	¯-4CI-3	36.4	552.7	0.76	1.21	0.0033	0.0075
¨-H12R-70	56.4	580.6	4.02	1.71	0.0053	0.0113	¯-4C1H-4	36.7	287.3	0.76	1.20	0.0026	-
-HSC-A-10	43.6	500.1	2.17	1.32	0.0037	0.0076	¯-4C6-5	35.0	481.5	2.27	1.64	0.0170	0.0250
-HSC-E-10	44.1	500.1	2.25	1.44	0.0041	0.0118	¯-4C6H-6	34.3	268.1	2.27	1.53	0.0093	0.0230
-HSC-F-10	48.1	500.1	2.24	1.43	0.0047	0.0184	¯-4A3-7	40.9	503.4	1.66	1.28	0.0044	0.0072
¨-HSC-A-08	43.1	500.1	1.74	1.22	0.0048	0.0057	¯-4A4-8	40.8	528.0	1.59	1.36	0.0057	0.0105
¨-HSC-B-08	48.5	500.1	1.74	1.27	0.0044	0.0070	¯-4A5-9	40.5	361.2	2.39	1.23	0.0050	0.0168
¨-HSC-E-08	43.6	500.1	1.76	1.29	0.0042	0.0077	¯-4A6-10	40.7	459.6	2.32	1.31	0.0103	0.0200
-HSC-A-12	46.1	436.4	3.09	1.41	0.0048	0.0103	¯-4C3-11	40.7	459.6	1.62	1.27	0.0051	0.0110
-HSC-B-12	47.1	436.4	2.98	1.53	0.0039	0.0172	¯-4C4-12	40.8	719.6	1.52	1.46	0.0205	0.0254
¨-HSC-E-12	49.0	500.1	2.70	1.68	0.0043	0.0184	¯-4A1-13	31.3	528.0	0.80	1.30	0.0045	0.0095
-USC-B-08	87.5	440.0	3.20	1.22	0.0049	0.0126	¯-2A5-14	31.5	448.7	2.39	1.38	0.0110	0.0205
-USC-C-08	87.0	440.0	3.16	1.26	0.0046	0.0125	¯-2A6-15	31.7	481.5	2.32	1.47	0.0215	0.0260
-USC-E-08	86.7	500.0	2.70	1.19	0.0048	0.0066	¯-2C1-16	32.5	667.6	0.76	1.36	0.0056	0.0123
-USC-F-08	86.5	500.0	2.85	1.23	0.0049	0.0065	¯-2C5-17	32.9	459.6	2.37	1.36	0.0157	0.0245
-USC-B-10	86.0	440.0	4.17	1.32	0.0044	0.0093	¯-2C6-18	33.1	528.0	2.27	1.70	0.0280	0.0300
-USC-B-10[A]	86.9	330.0	3.70	1.24	0.0045	0.0094	¯-4B3-19	33.4	459.6	1.80	1.43	0.0061	0.0090
-USC-C-10	87.5	440.0	3.95	1.29	0.0048	0.0067	¯-4B4-20	34.7	517.1	1.70	1.52	0.0080	0.0155
-USC-C-10[B]	86.3	330.0	3.51	1.29	0.0033	0.0065	¯-4B6-21	35.5	481.5	2.40	1.54	0.0144	0.0250
¨-USC-E-10	86.8	440.0	4.05	1.30	0.0049	0.0109	¯-4D3-22	35.5	459.6	1.60	1.44	0.0041	0.0097
¨-USC-E-10[C]	86.5	500.0	3.38	1.28	0.0059	0.0085	¯-4D4-23	35.9	517.1	1.70	1.54	0.0076	0.0165
-USC-F-10	85.9	440.0	4.18	1.31	0.0069	0.0083	¯-4D6-24	35.9	481.5	2.30	1.63	0.0177	0.0246
-USC-B-12	86.3	440.0	4.63	1.35	0.0065	0.0208	¯-HC-7-8B1	75.0	539.5	2.61	1.25	0.0036	0.0046
-USC-C-12	85.8	440.0	4.74	1.33	0.0072	0.0141	¯-HC-7-8C1	75.0	539.5	2.97	1.35	0.0033	0.0056
-USC-E-12	86.0	440.0	4.98	1.34	0.0091	0.0162	¨ Chung, ¯ Shin, ¯ Lee, ¨ Sheikh, ¯ Lim						

Where, ε_{c50c} is calculated from Eq. (6), Cusson and Paultre (1995),[12] as the least absolute deviations method. Substituting Eq. (4) into Eq. (3), the strain corresponding to 50% of peak stress can be calculated;

$$\varepsilon_{c50c} = 0.004 + 0.15(f_{le} / f_{co})^{1.1} \quad (6)$$

Substituting Eq. (1) into Eq. (7), the strain corresponding to 50% of peak stress can be modified calculated;

$$f_{le} = K_e f_l = \frac{K_e f_{hcc}}{s}\left(\frac{A_{shx} + A_{shy}}{b_c + d_c}\right) \quad (7)$$

To quantify the response of columns, it is desirable to define response index that quantitatively describe the columns' behavior. The ductility of the column depends greatly on the confinement degree of the core concrete. The failure of the column is conventionally defined at the maximum tip displacement of column, where the remaining capacity of the column has dropped to 85% of the peak load. So the value of ε_{c85c} is the essential parameter that describe columns' behavior.

The strain, ε_{c50c} corresponding to 50% of the maximum confined concrete strength on the stress-strain curve gives the additional ductility due to rectangular hoops. When analyzing the results of the three investigations [13, 14, 15], it was assumed that the cover concrete had spalled away by the time stress had fallen to 50% of the maximum stress. So the value of ε_{c50c} defines the additional ductility that define columns' behavior. To apply both ε_{c85c} and ε_{c50c}, this proposed model considers the value of ε_{c675c}. The descending slope of this segment is defined by the strain corresponding to 67.5% of peak stress, and the value of ε_{c675c} is the mean point between the value of ε_{c85c} and ε_{c50c}.

$$\varepsilon_{c675c} = \frac{\varepsilon_{c85c} + \varepsilon_{c50c}}{2} \quad (8)$$

2.4 Proposed constitutive model for confined HSC

Fig. 2 shows the proposed complete stress-strain curve of confined HSC in a member. The parabolic ascending branch and bilinear descending branches are used to simu-

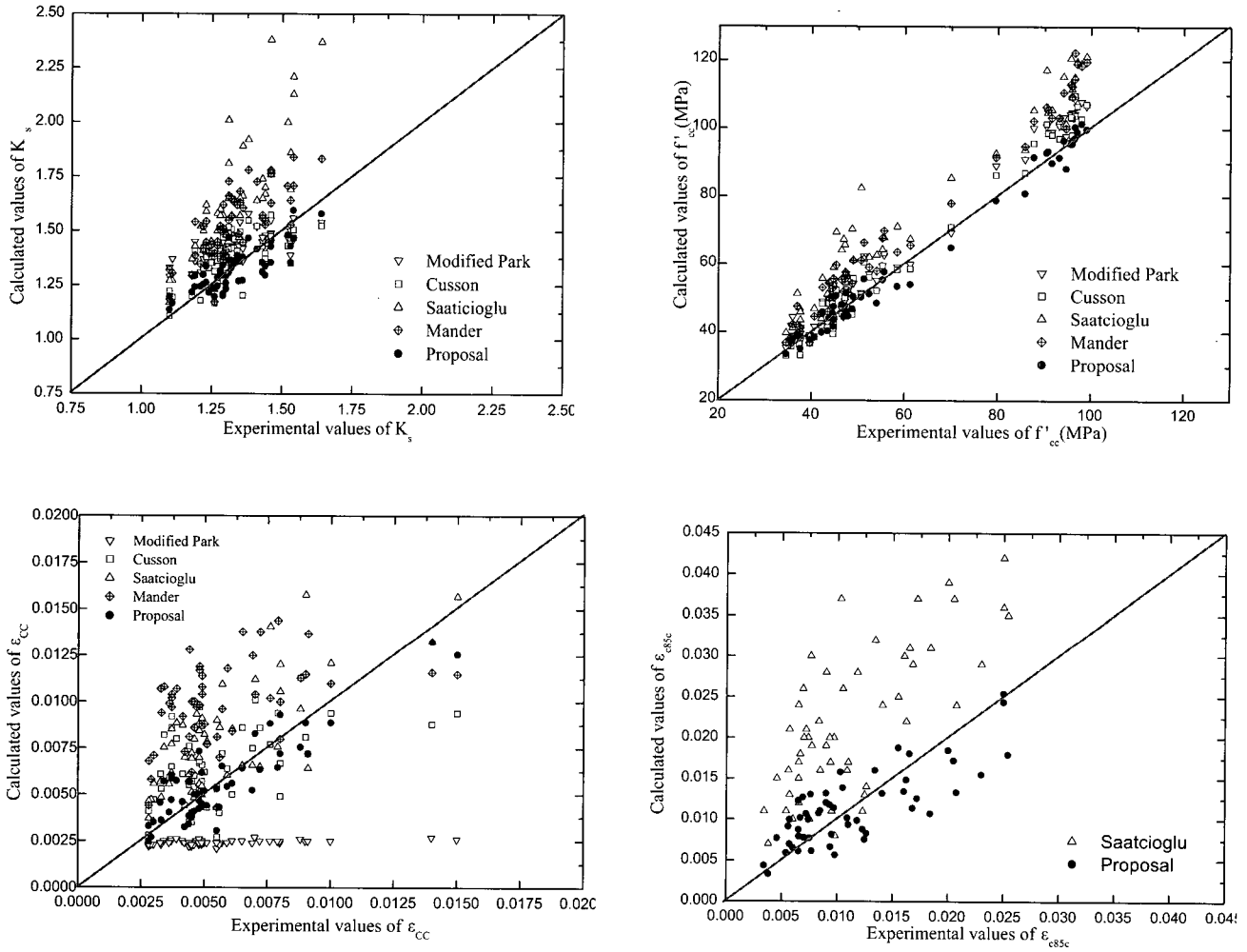

Fig. 1 Comparison of the calculated and experimental values; (a), K_S (b), f'_{cc} (c), ε_{cc} (d), ε_{C85C}

-late a complete stress-strain curve of a confined concrete in this study (Fig. 2). The ascending part (OA) is a relationship originally proposed by Popovics (1973)[16] for concrete and written as Eq. (9). Where, k controls the initial slope and the curvature of the ascending branch and can be derived as Eq. (10). For HSC, the coefficient k is large and expresses the fact that the ascending branch is nearly linear with a high elastic modulus.

$$f_c = f'_{cc}\left[\frac{k\left(\varepsilon_c/\varepsilon_{cc}\right)}{k-1+\left(\varepsilon_c/\varepsilon_{cc}\right)^k}\right], \qquad \varepsilon_c \le \varepsilon_{cc} \tag{9}$$

$$k = \frac{E_c}{E_c - \left(f'_{cc}/\varepsilon_{cc}\right)}, \qquad E_c = 9500(f_{ck})^{0.3}\ (MPa) \tag{10}$$

The stress-strain relation of the first descending part AC can be determined by;

$$f_c = f'_{cc} + X(\varepsilon_{cc} - \varepsilon_c), \quad \varepsilon_{cc} \le \varepsilon_c \le \varepsilon_{c20c} \tag{11}$$

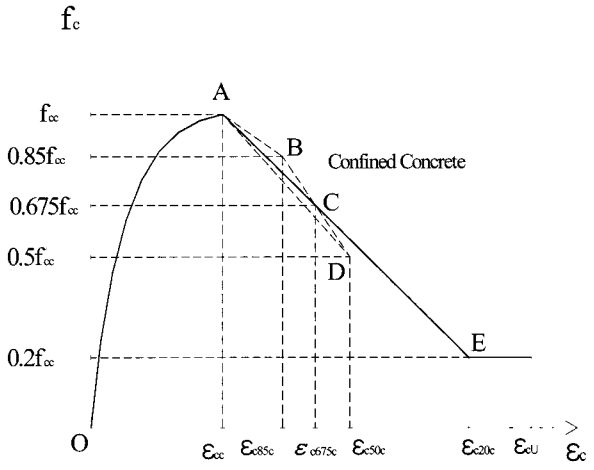

Fig. 2 Stress-strain curve of confined HSC

Where X is the slope of the first descending curve and can be defined as;

$$X = \frac{0.325 f'_{cc}}{\varepsilon_{c675c} - \varepsilon_{cc}} \tag{12}$$

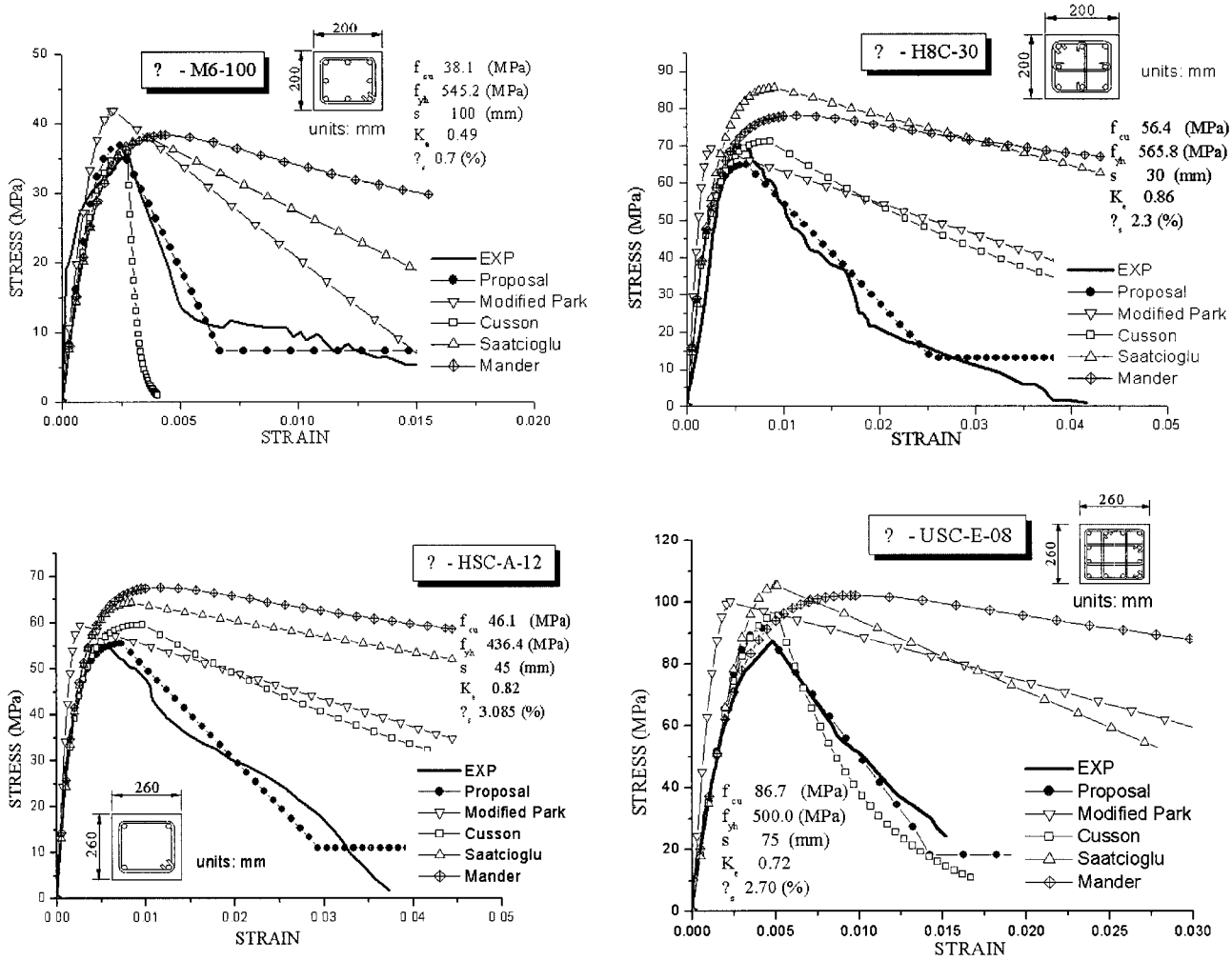

Fig. 3 Comparison of stress-strain for HSC columns

2.5 Ultimate concrete compressive strain

In order to calculate the available ultimate rotation capacity at a plastic hinge in a reinforced concrete flexural member, it is necessary to be able to predict the ultimate concrete compressive strain ε_{cu}. The useful limit occurs when transverse confining steel fractures, which may be estimated by equating the strain-energy capacity of the transverse steel at fracture to the increase in energy absorbed by the concrete. Where, ε_{cu} was proposed by T. Paulay and M.J.N. Priestly (1992)[17]. A conservative estimate for ultimate compression strain is given by Eq. (13). Where, ε_{sm} is the steel strain corresponding to the peak tensile stress and ρ_s is the volumetric ratio of confining steel.

$$\varepsilon_{cu} = 0.004 + 1.4\frac{\rho_s f_{yh}\varepsilon_{sm}}{f'_{cc}} \tag{13}$$

3. Stress-strain curve for unconfined HSC

This relationship is used for unconfined cover concrete, as well as the entire column section when confinement is negligible. The following expressions are used to describe the stress-strain relationships for unconfined concrete. Armen Martirossyan (1998)[18] has conducted tests on circular and square high-strength reinforced concrete columns. This model assumes the ultimate strain of unconfined concrete is 0.005.

4. Application model for steel reinforcement

The stress-strain relationship used for reinforcing steel in tension consists of three segments. The elastic and yield portions of the curve are linear and form a bilinear relationship. The strain-hardening portion is represented by a parabolic curve and follows the yield segment, as illustrated in Fig. 4. Mander et al. (1984)[19] found that the stress-strain curve in the strain hardening region ($\varepsilon_{sh} \le \varepsilon_s \le \varepsilon_{su}$) can be predicted with good accuracy by;

$$f_s = f_{su} - (f_{su} - f_y)\left(\frac{\varepsilon_{su} - \varepsilon_s}{\varepsilon_{su} - \varepsilon_{sh}}\right)^P \tag{14}$$

$$P = E_{sh}\left(\frac{\varepsilon_{su} - \varepsilon_{sh}}{f_{su} - f_y}\right)^P \tag{15}$$

Where ε_s is the steel strain; ε_{sh} is the steel strain at commencement of strain hardening; ε_{su} is the steel strain at f_{su} ; f_{su} is the ultimate tensile strength of steel; f_y is the yield strength of steel; E_{sh} is the strain-hardening modulus of steel; and strain rate is taken into account by using values for the control parameters that correspond to the relevant strain rate.

5. Application model for concrete in tension

5.1 Tension stiffening in plain concrete

Concrete can be considered as an elastic strain softening material in tension. The problem with this concept is the extent which the tension stiffening can be incorporated. Alternatively concrete can be assumed to be elastic-brittle in tension. The general strain softening model for concrete

$$\sigma = f_{cr}\{\exp[-(\varepsilon - \varepsilon_{cr})/\alpha]\} \tag{16}$$

is given by Perterson (1981)[20] as a bilinear curve. The stress σ is defined as;

Where ε is the nominal tensile strain in the cracked

$$\alpha = \left(G_F - \frac{1}{2}f_{cr}\varepsilon_{cr}l_{ch}\right) > 0 \tag{17}$$

$$l_{ch} = \frac{volume\ containing\ a\ crack}{area\ of\ crack} = \frac{V}{A_{cr}} \approx (dV)^{1/3} \tag{18}$$

zone, ε_{cr} is the cracking, and α, the softening parameter, is given by

5.1.1 Fracture energy and characteristic length

The fracture mode of concrete subjected to tension allows the application of fracture mechanics concepts. The fracture energy is defined as the energy required propagating a tensile crack of unit area. As a rough approximation fracture energy may be estimated from the compressive strength of concrete tasking into account the maximum aggregate size as expressed by Eq. (19) from CEB-FIP MC. 90[21]. Because of substantial increase of concrete brittleness at higher strength grades it has been proposed to limit fracture energy for f_{ctm} >80 MPa to a constant value as given by Eq. (20).

$$G_F = G_{Fo}\left(\frac{f_{cm}}{f_{cmo}}\right)^{0.7} \quad for\ f_{cm} \le 80MPa \tag{19}$$

$$G_F = 4.30G_{Fo} \quad for\ f_{cm} > 80MPa \tag{20}$$

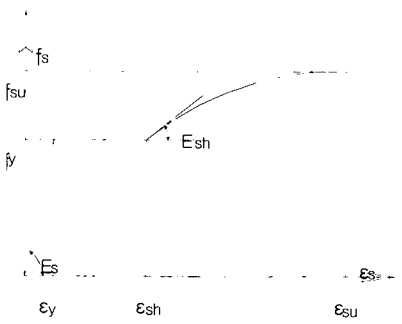

Fig. 4 Steel stress-strain model

length of a specimen subjected to axial tension in which just enough elastic strain is stored to create one complete fracture surface. Thus, a decrease of characteristic length is an indication of increased brittleness.

$$l_{ch} = \frac{E_{ci} G_F}{f_{cr}^2} \tag{21}$$

Where l_{ch} is the characteristic length [mm]; E_{ci} is the modulus of elasticity [MPa]; G_F is the fracture energy [N/mm]; G_{Fo} is the base value of fracture energy which depends on maximum aggregate size d_{max} as given in CEB-FIP MC. 90.

5.2 Tension stiffening in reinforced concrete

In order to predict accurately the post-cracking behavior of reinforced concrete elements, Collins (1991)[22] found that it was necessary to account for the average tensile stress which still exits in the concrete between cracks. To allow for this "tension stiffening" effect he specified a gradual unloading branch instead of an abrupt drop to zero stress level for the relationship of concrete.

$$0 \le \varepsilon_1 \le \varepsilon_{cr} \quad \sigma_1 = E_c \varepsilon_1 \tag{22}$$

$$\varepsilon_1 > \varepsilon_{cr} \quad \sigma_1 = \frac{f_{cr}}{1 + \sqrt{500 \varepsilon_1}} \tag{23}$$

5.3 Relations between tensile strength and compressive strength

Various relations have been proposed to estimate the axial tensile strength of concrete form its compressive strength. Eq. (30) is based on more recent data including also tests on high-strength concretes by the CEB-FIP MC. 90.[21]

$$f_{cr} = f_{ctmo} \ln(1 + f_{cm} / f_{cmo}) \tag{24}$$

Where f_{cr} is the mean axial tensile strength [MPa.]; f_{cm} is the mean compressive strength [MPa.]; f_{ctmo} is 2.12 MPa; f_{cmo} is 10 MPa.

6. Fiber section analysis

A computer program was developed to carry out calculations for theoretical moment-curvature relations of the test specimens using the concrete stress-strain curves from the proposed model described previously. The required input data included cross-sectional dimensions of specimens, position, and amount of longitudinal steel including the location of laterally supported longitudinal bars, properties of longitudinal steel, the stress-strain of confined concrete, the stress-strain of unconfined concrete, and applied axial load. The "fiber section analysis" is a numerically intensive method for determining the cross strength and stiffness of member cross sections. In the fiber model, the cross section is discredited into many small regions where the constitutive relationships are based on stress-strain model and each region represents a fiber of material running longitudinally along the member. The method assumes plane sections to remain plane, thus implying full compatibility between the confined concrete and unconfined concrete components of cross section.

7. Moment-curvature relationship

A finite approach used to compute the moment-curvature relationship numerically in which the concrete and the steel areas. The program first calculates moment and curvature at cracking. Beyond cracking, the analysis is conducted for different values of extreme compressive fiber strain. The strain profile is established for each value of fiber strain and assumed location of neutral axis. The sectional analysis continues until rather the tension steel reaches its ultimate fracturing stress, or the extreme compressive fiber strain reaches to a limiting value specified in the input.

7.1 Comparison of test data with analytical results

Fig. 6 shows the experimental and analytical moment curvature relations for four of the columns tested[23]. The light lines indicate cyclic experimental results, and the heavy lines indicate the monotonic envelopes generated by the proposed models.

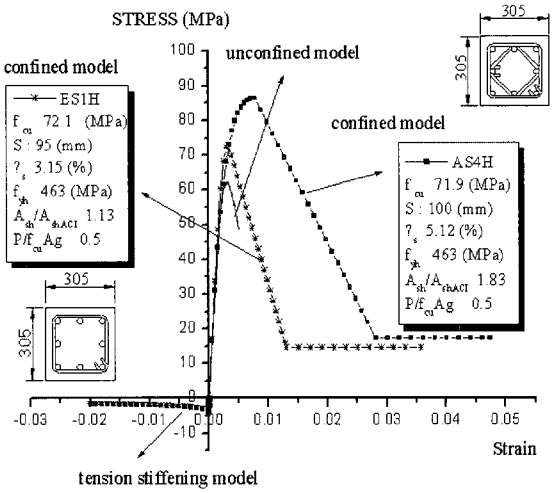

Fig. 5 Analytical stress-strain curves

Both the experimental and analytical moment curvature relations exhibit a well-defined yield point followed by a nearly horizontal yield plateau. The yield moment and curvature are predicted with reasonable accuracy. The initial experimental stiffness tended to be slightly greater than predicted by the moment curvature model because the model assumes that the concrete is always cracked.

7.2 Parametric studies on moment-curvature relation

Parametric studies are performed examine the effects of constituent material properties as well as topological arrangement of reinforcements on moment-curvature relationships. It has been analytically observed that ductility of high-strength concrete columns is influenced mostly by magnitude of the axial load and spacing or volumetric ratio of lateral ties or yield strength of transverse reinforcement.

7.2.1 Effect of axial load

Fig. 7 shows the comparisons of moment-curvature envelop for two groups of columns with the same reinforcement configurations and material strength, but different axial load levels. This figure indicates that, if the axial-load level has a beneficial influence on the moment resisting capacity, it has a negative effect on the inelastic flexural behavior of the column. Higher axial-load ratio of $0.5f_{cu}A_g$ and $0.6f_{cu}A_g$ resulted in an increase in the rate of stiffness degradation and adversely affected the performance of HSC columns. These results underlined the need to incorporate the level of axial load in computing the required amount of confining steel.

7.2.2 Effect of volumetric ratio of lateral ties

Fig. 8 shows the effect of volumetric ratio of lateral ties on the moment-curvature curve. This program points to the influence of the volumetric ratio of confinement steel as a main parameter in controlling column response. As was stated previously, however, the level of axial load is also very important. For practical applications, the requirement for the volumetric ratio of transverse steel should be related to the axial-load ratio. For the columns calculated in this research program, a volumetric ratio of confinement steel of approximately 2% seems acceptable to ductile behavior under an axial load less than or equal to $0.3f_{cu}A_g$ of axial-load capacity. For an axial load ratio of $0.5f_{cu}A_g$, a volumetric ratio of confinement steel of 6% seems adequate.

7.2.3 Effect of yield strength of transverse bar

Fig. 9 shows the results of two columns that could be compared for of yield strength of transverse reinforcement.

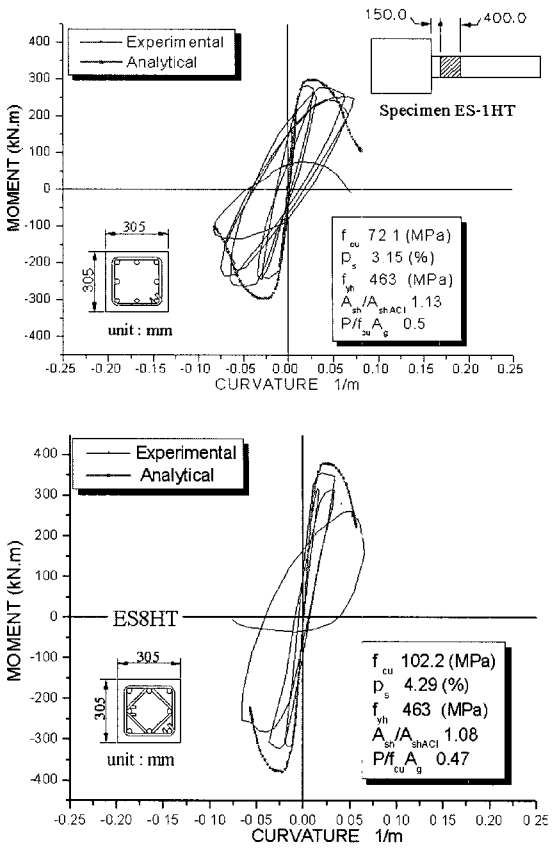

Fig. 6 Comparisons of moment-curvature curves

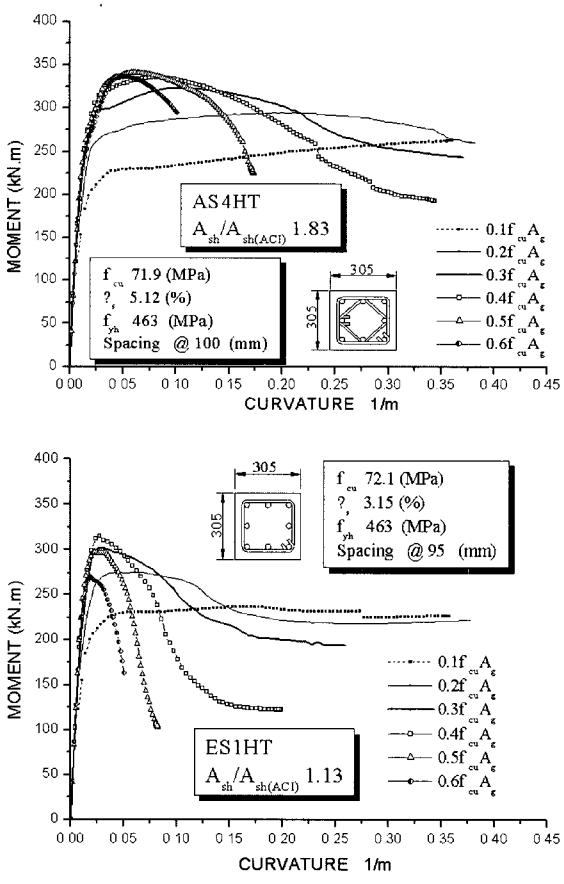

Fig. 7 Effect of ratio of axial load on moment-curvature relations

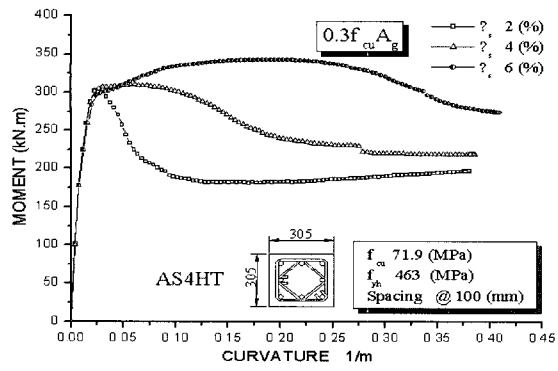

Moment-curvature relations ($P = 0.3f_{cu}A_g$)

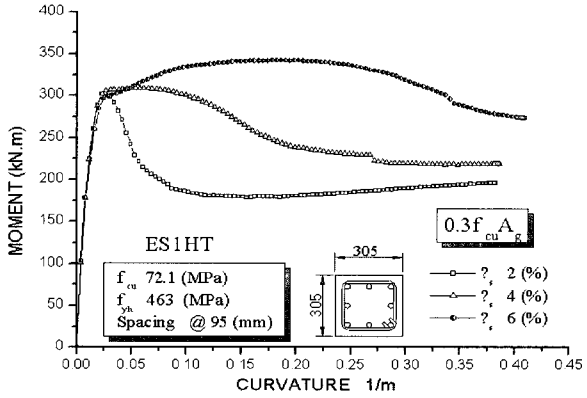

Moment-curvature relations ($P = 0.3f_{cu}A_g$)

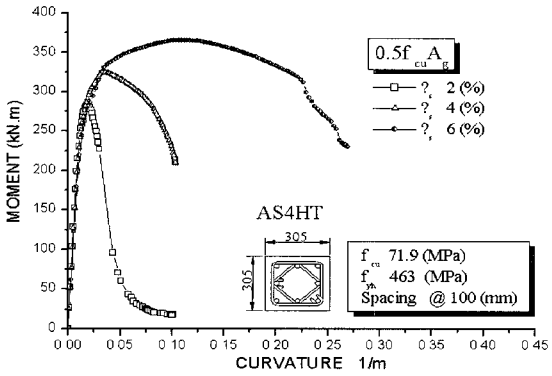

Moment-curvature relations ($P = 0.5f_{cu}A_g$)

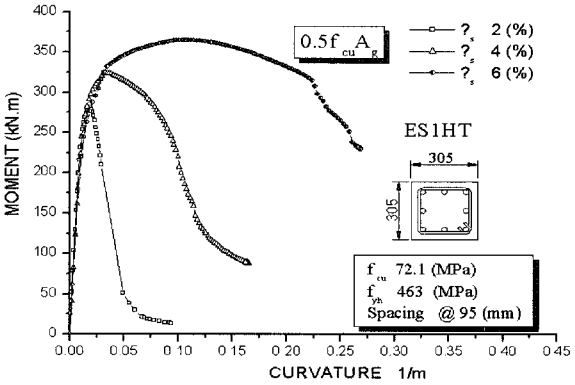

Moment-curvature relations ($P = 0.5f_{cu}A_g$)

Fig. 8 Effect of volumetric ratio of transverse reinforcement on moment-curvature relations

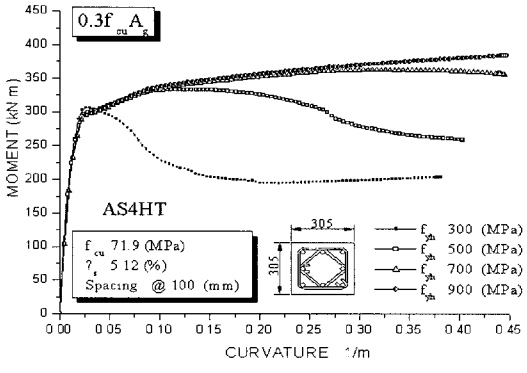

Moment-curvature relations ($P = 0.3f_{cu}A_g$)

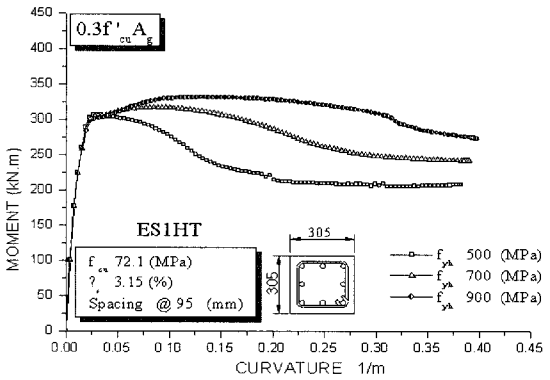

Moment-curvature relations ($P = 0.3f_{cu}A_g$)

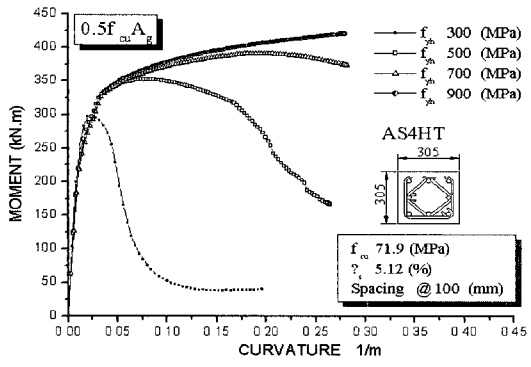

Moment-curvature relations ($P = 0.5f_{cu}A_g$)

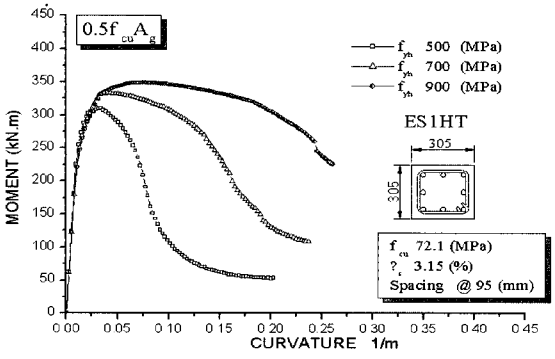

Moment-curvature relations ($P = 0.5f_{cu}A_g$)

Fig. 9 Effect of yield strength of transverse reinforcement on moment curvature relations

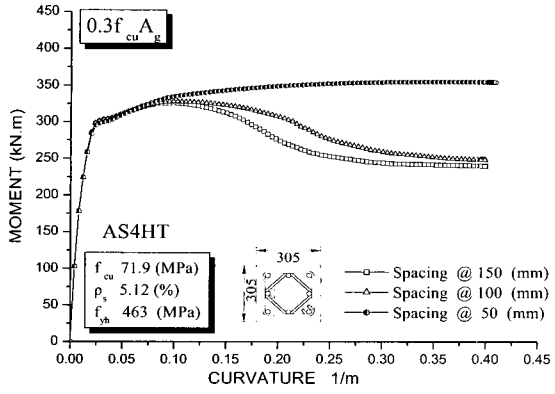

Moment-curvature relations ($P = 0.3f_{cu}A_g$)

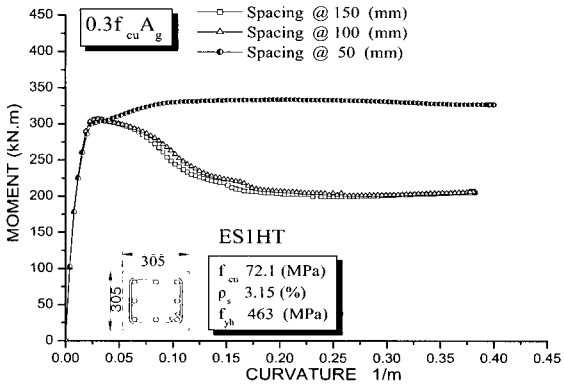

Moment-curvature relations ($P = 0.3f_{cu}A_g$)

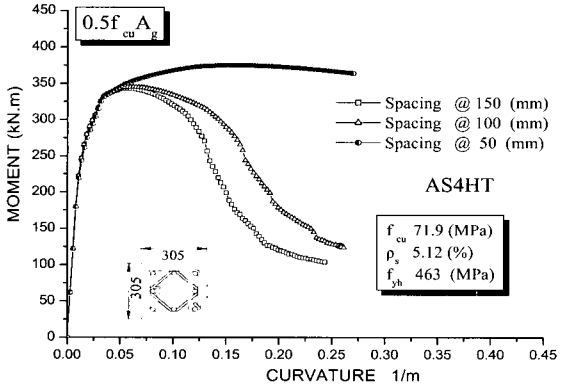

Moment-curvature relations ($P = 0.5f_{cu}A_g$)

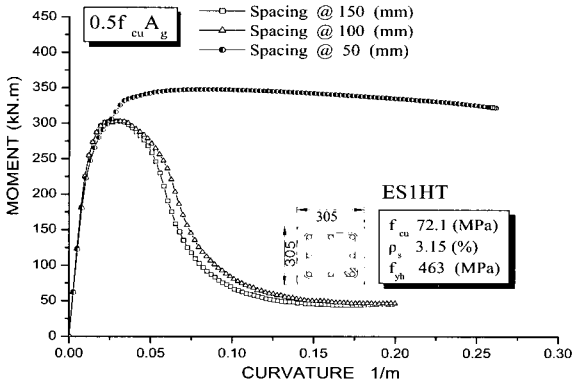

Moment-curvature relations ($P = 0.5f_{cu}A_g$)

Fig. 10 Effect of tie spacing on moment-curvature relation

The comparisons show in Fig. 9 indicate that columns confined with confined with 700MPa and 900MPa lateral steel showed improved strength and ductility when compared with compared with compared with those with 300MPa and 500MPa steel. Results indicate that at an axial load ratio of $0.5f_{cu}A_g$, increasing the yield strength of the transverse reinforcement has on the moment resisting capacity.

7.2.4 Effect of spacing

Fig. 10 shows the results of two columns that could be compared for effect of transverse reinforcement spacing. As was stated previously, however, the level of axial load is also very important. Results indicate that at an axial load ratio of $0.5f_{cu}A_g$, decreasing the transverse reinforcement spacing has on the moment resisting capacity.

8. Summary and conclusions

The strength and flexural ductility of HSC columns have been investigated using a fiber element model incorporating nonlinear constitutive models accurate for high-strength concrete. The accuracy of the analysis has been substantiated comparisons to tests of HSC columns subjected to axial forces and HSC columns subjected to axial compressive and cycle lateral loads. On the basis of the analytical studies, the following conclusions were drawn.

1) This model is applicable to high-strength concrete, covering a strength range between 40MPa and 90MPa. The developed HSC model is shown to superior to other models in predicting test results of the compressive stress-strain curves of the confined high-strength concrete under concentric load.
2) A series of models for predicting the behavior of confined high-strength concrete columns is proposed as part of a potential improved design process. The series of detailed models predicted moment-curvature of cantilevers confined high-strength concrete columns reasonably well.
3) Based on the parametrical researches, the following conclusions and recommendations are presented.

(1) This research presents that, if the axial-load level has a beneficial influence on the moment resisting capacity, it has a negative effect on the inelastic flexural behavior of the column.

(2) For parametrical applications, the requirement for the volumetric ratio of transverse steel should be related to the axial-load ratio. When the columns are subjected to a high axial load ratio, a significant amount of lateral steel is necessary.

(3) This parametrical results present that at an high axial load ratio of $0.5f_{cu}A_g$, increasing the yield strength of the transverse reinforcement has on the moment resisting capacity. Ratios exceeding 4% will be difficult to use in practice. High-yield strength steel may be a solution to reduce the quantities required. New equations should be developed that take into account high-strength transverse steel and axial-load ratio.

Notation

b_c = side dimension of concrete core parallel to x-axis;

d_c = side dimension of concrete core parallel to y-axis;

A_{shx} = total cross-section area transverse reinforcement perpendicular to x-axis;

A_{shy} = total cross-section area transverse reinforcement perpendicular to y-axis;

E_c = modulus of elasticity of plain concrete;

$E_{\sec}$ = secant modulus at the peak strength of confined concreter;

E_{sh} = the strain-hardening modulus of steel;

f_c = stress in concrete;

f_{ck} = the compressive cylinder strength of unconfined concrete;

f_{co} = unconfined concrete compressive strength in member;

f_{cc}' = maximum compressive strength of confined concrete in a member;

f_l = nominal lateral pressure applied on the concrete core;

f_{le} = effective confinement pressure applied on the concrete core;

f_{lex}, f_{ley} = equivalent lateral pressure perpendicular to b_{cx} and b_{cy}, respectively;

f_{hcc} = stress in ties at maximum strength of concrete;

f_{yh} = yield strength of transverse reinforcement;

f_y = yield strength of steel;

f_{su} = ultimate tensile strength of steel;

f_{cr} = tensile strength of concrete;

f_{ctmo} = tensile strength of concrete;

f_{cm} = mean compressive strength;

G_F = fracture energy;

G_{Fo} = base value of fracture energy which depends on maximum aggregate size d_{max} as given CEB-FIP MC. 90;

α = softening parameter;

K_s = strength enhancement coefficient;

K_e = confinement effectiveness coefficient;

l_{ch} = characteristic length;

s = spacing of transverse reinforcement;

s' = clear vertical spacing between the stirrups;

ε_c = concrete strain;

ε_{co} = axial strain in plain concrete corresponding to f_{co};

ε_{cc} = strain corresponding to peak stress of confined concrete;

ε_{c85c} = strain corresponding to 85% of peak stress of confined concrete on descending branch;

ε_{c50c} = strain corresponding to 50% of peak stress of confined concrete on descending branch;

ε_{c675c} = strain corresponding to 67.5% of peak stress of confined concrete on descending branch;

ε_{cu} = ultimate strain of concrete;

ε_{cr} = strain at cracking;

ε_s = steel strain;

ε_{sh} = steel strain at commencement of strain hardening;

ε_{su} = steel strain at the ultimate tensile strength of steel;

ε_{sm} = the steel strain at maximum tensile stress;

ω_i = clear horizontal spacing between longitudinal bars;

ρ_{sl} = the ratio of longitudinal steel area to the total core area;

ρ_s = volumetric ratio of lateral ties;

References

1. ACI-ASCE Committee 441, "High-Strength Concrete Columns; State of the Art," *ACI Structural Journal*, Vol.94, No. 3, May-June 1997, pp.323~335.
2. SPSS Program User's Mannual.
3. Heon-Soo Chung and Nam-Joo Kim, "*An experimental study on behavior of high-strength concrete column according to amount of tie*," Dept. of architectural engineering, University of Chung-Ang, Seoul, ON, Korea, 1997.
4. Heon-Soo Chung and Young-in Lee, "*An experimental study on the strength and ductility of high-strength reinforced concrete column according to the configuration of ties*," Dept. of architectural engineering, University of Chung-Ang, Seoul, ON, Korea, 1998.
5. Sung–Woo Shin and Beom–Seok Han, "Confined model of high-strength reinforced concrete tied columns," *Proceedings of the Korea Concrete Institute*, Vol.14, NO.1, 2002. 5, pp.923~928.
6. Sung-Woo Shin and Beom-Seok Han, "Confinement effects of high strength reinforced concrete tied columns," *Journal of the Korea Concrete Institute*, Vol.14, No.4 (Serial No.70), 2002, pp.578~588.
7. Li-Hyung Lee and Kang-Kun Lee, "*Strength and ductility confined high-strength concrete columns under uniaxial loads*," Dept. of architectural engineering, University of Hanyang, Seoul, on, Korea, 1990.

8. Sheikh, S. A. and Uzumeri, S. M., "Strength and ductility of tied concrete columns," *Journal of Structural Engineering*, Vol.106, No.5, 1980, pp.1079~1102.
9. Gyoung-Teag Lim, "*Ductility and strength of high-strength concrete columns under uniaxial loads*," Dept. of architectural engineering, Chungnam National University, Daejeon, 1992.
10. Soliman, M.T.M. and Yu, C.W., "The Flexural Stress-Strain Relationships for Concrete Confined in Rectangula Transverse Reinforcement," *Magazine of Concrete Research* (London), Vol.19, No.61, Dec, 1967, pp.223~238.
11. "Setunge S. Structural Properties of Very High Strength concrete," PhD. thesis, Monash University, Australia, 1993.
12. Cusson, D. and Paultre, P., "High-strength concrete columns confined by rectangular ties," Journal of Structural Engineering, Vol.120, No.3, 1994, pp.783~804.
13. V. V. Bertero and C. Felippa, Discussion of "Ductility of Concrete," by H. E. H. Roy and M. A. Sozen, Proceedings of the International Symposium on Flexural Mechanics of Reinforced Concrete, *ASCE-ACI*, Miami, November 1964, pp.227~234.
14. H. E. H. Roy and M. A. Sozen, "Ductility of Concrete," *Proceedings of the International Symposium on Flexural Mechanics of Reinforced Concrete, ASCE-ACI*, Miami, November 1964, pp.213~224.
15. M. T. M Soliman and C.W. Yu, "The flexural stress-strain relationship of concrete confined by rectangular transverse reinforcement," *Magazine of Concrete Research*, Vol.19, No.61, December 1967, pp.223~238.
16. Popovics, S., "Analytical approach to complete stress-strain curves," *Cement and Concrete Res.*, Vol.3, No.5, 1973, pp.583~599.
17. T. Paulay and M. J. N. Priestly, "Seismic Design of Reinforced Concrete and Masonry Buildings," John Willey & Sons, INC, 1992.
18. Armen Martirossyan, "Performance of reinforced high-strength concrete columns," *Dept. of civil engineering*, University of Southern California, 1998.
19. Mander, J. B., Priestly, M. J .N, and Park, R., "*Seismic design of bridge piers*," Res. Rep. 84-2, Dept. of Civil Eng. Univ. of Canterbury, Christchurch, New Zealand, 1984.
20. Peterson, J., "*Crack growth and development of fracture zones in plain concrete and similar materials*," Phd. Thesis, University of Lund, 1981.
21. Textbook on Behaviour, "Design and Performance Updated knowledge of the CEB-FIP MC,"Vol.1, 1990.
22. Michael P. Collins and Denis Mitchell, "*Prestressed Concrete Structures*," Prentice-Hall, Inc., 1991, 347pp.
23. Oguzhan Bayrak and Shamim A. Sheikh, "Confinement reinforcement design considerations for ductile HSC columns,"□*Journal of Structural Engineering*, Vol.124, No.9, September, 1998.